

Advanced Technologies for Neuro-Motor Assessment and Rehabilitation  
(Monte San Pietro, 18th – 24th June 2006)

# Methods of sensory information processing for inertial sensing in human movement studies

Angelo Maria Sabatini



Scuola Superiore Sant'Anna,  
Pisa, Italy

Bologna, 20th June 2006

## Outline of the talk

- Introductory remarks
- Mathematical preliminaries
- Strap-down inertial navigation in human movement analysis
- Sensor modeling, calibration, and signal processing
- Dead-reckoning approaches for pedestrian navigation (current research at ARTS Lab-SSSA)

## Introductory remarks

### Background – 1

- Inertial sensors are position, attitude or motion sensors the references of which are completely internal, except possibly for initialization (alignment).\*
- They measure physical quantities, such as linear accelerations and angular velocities of the **body** to which they are strapped.






\* Curey, R.K., Ash, M.E., Thielman, L.O., Barker, C.H. (2004). Proposed IEEE inertial systems terminology standard and other inertial sensor standards. *IEEE Position Location and Navigation Symposium, PLANS 2004*, Monterey, CA, U.S.A., 26-29 April, 83-90.

## Background – 2

- Inertial sensors are position, attitude or motion sensors the references of which are completely internal, except possibly for initialization (alignment).
- An inertial measurement unit (IMU) contains multiple inertial sensors (accelerometers and/or gyroscopes) in fixed orientations relative to one another.

## Background – 3

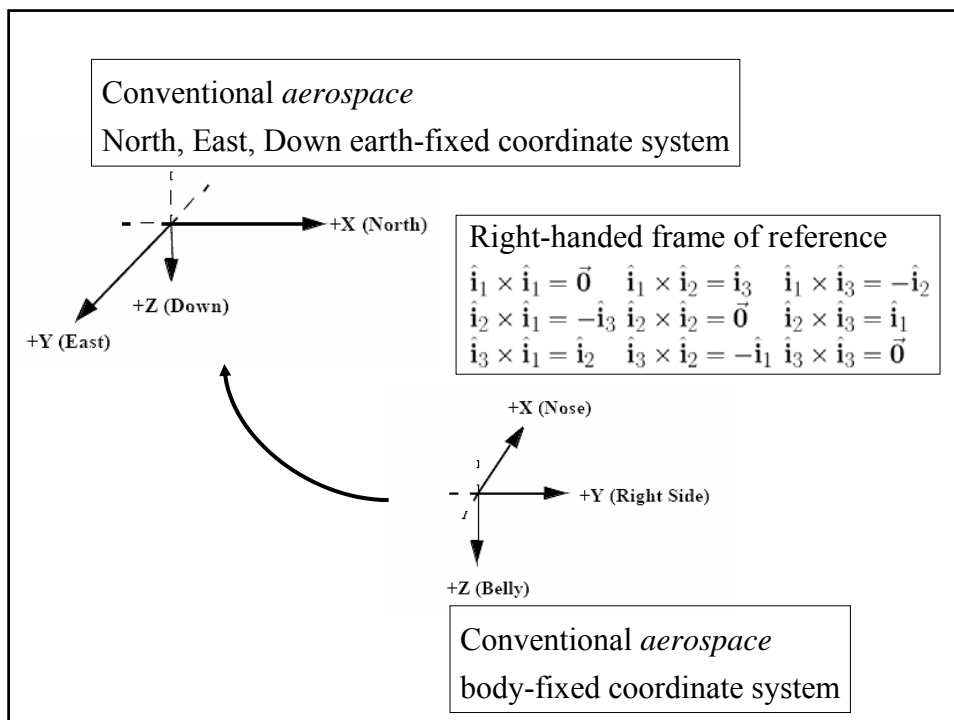
- Using the outputs from an IMU, an inertial navigation system (INS) estimates a body's position and orientation, in connection with a gravitational field model and the operation of a reference clock.
- Using a geomagnetic field model, magnetic sensors can help specifying the absolute location of an INS during initialization, and mitigating the INS error growth during operation.

<p><b>Motion analysis</b></p> 	<p><b>Aeroplanes</b></p> 	<p><b>Spacecrafts</b></p> 	<p><b>Robots</b></p> 
<p>Video-motion sensing, infrared, magnetic, ultrasound and GPS technologies are <u>externally referenced</u>.</p>	<p>Inertial sensors (accelerometers and gyros), are <u>internally referenced</u>, i.e. they sense their own (change of) position and orientation.</p>		
	<p><b>Motion analysis</b></p> 	<p>Inertial sensors are increasingly popular, due to low-cost, small size, light weight, limited power requirements.</p>	

# Mathematical preliminaries

## Determining twist and pose of a rigid body

- Choose a coordinate system attached to an appropriate inertial frame, and express all vectors in component form relative to these coordinates.
- For motion on or near the surface of the earth at speeds far below orbital velocity, a commonly used inertial frame is the local “flat Earth” system (origin arbitrarily located, and coordinate axes directed in the local north, east and down directions).



## The Direction Cosine Matrix

- It performs the coordinate transformation of a vector resolved in the reference frame,  ${}^E \mathbf{x}$  into a vector resolved in the body frame,  ${}^B \mathbf{x}$ .
- Leonhard Euler (1707-1783) proposed that the rotation from one frame to another can be visualized as a sequence of three simple rotations about base vectors.
- Euler angle rotations are often defined w.r.t. body-fixed axes rather than earth-fixed axes.

$$\mathbf{R}_x(\varphi) = \begin{bmatrix} 1 & 0 & 0 \\ 0 & \cos \varphi & \sin \varphi \\ 0 & -\sin \varphi & \cos \varphi \end{bmatrix}$$

$$\mathbf{R}_y(\theta) = \begin{bmatrix} \cos \theta & 0 & -\sin \theta \\ 0 & 1 & 0 \\ \sin \theta & 0 & \cos \theta \end{bmatrix}$$

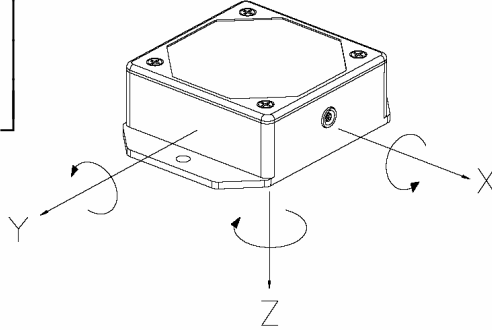
$$\mathbf{R}_z(\psi) = \begin{bmatrix} \cos \psi & \sin \psi & 0 \\ -\sin \psi & \cos \psi & 0 \\ 0 & 0 & 1 \end{bmatrix}$$

**DCM**

$${}^B \mathbf{x} = \mathbf{R}_x(\varphi) \mathbf{R}_y(\theta) \mathbf{R}_z(\psi) {}^E \mathbf{x}$$

$${}^E \mathbf{x} = \mathbf{R}_z(\psi) \mathbf{R}_y(\theta) \mathbf{R}_x(\varphi) {}^B \mathbf{x}$$

$$\text{DCM} = \begin{bmatrix} C_{11} & C_{12} & C_{13} \\ C_{21} & C_{22} & C_{23} \\ C_{31} & C_{32} & C_{33} \end{bmatrix}$$



$$\text{DCM} = \begin{bmatrix} C_{\theta}C_{\psi} & C_{\theta}S_{\psi} & -S_{\theta} \\ S_{\phi}S_{\theta}C_{\psi} - C_{\phi}S_{\psi} & S_{\phi}S_{\theta}S_{\psi} + C_{\phi}C_{\psi} & S_{\phi}C_{\theta} \\ C_{\phi}S_{\theta}C_{\psi} + S_{\phi}S_{\psi} & C_{\phi}S_{\theta}S_{\psi} - S_{\phi}C_{\psi} & C_{\phi}C_{\theta} \end{bmatrix}$$

## The angular velocity vector – 1

Let the angular rate of a rigid body measured in body coordinates  ${}^B \boldsymbol{\omega} = [p \ q \ r]^T$  and  $\dot{\phi}, \dot{\theta}, \dot{\psi}$  the corresponding Euler angle rates of the body. The angular velocity in earth coordinates is then

$${}^E \boldsymbol{\omega} = \begin{bmatrix} \omega_x \\ \omega_y \\ \omega_z \end{bmatrix} = \begin{bmatrix} 0 \\ 0 \\ \dot{\psi} \end{bmatrix} + \mathbf{R}_z(\psi) \begin{bmatrix} 0 \\ \dot{\theta} \\ 0 \end{bmatrix} + \mathbf{R}_z(\psi)\mathbf{R}_y(\theta) \begin{bmatrix} \dot{\phi} \\ 0 \\ 0 \end{bmatrix}$$

$$\downarrow$$

$${}^B \boldsymbol{\omega} = \mathbf{R}_x(\phi)\mathbf{R}_y(\theta)\mathbf{R}_z(\psi) {}^E \boldsymbol{\omega}$$

## The angular velocity vector – 2

The system of differential equations describing the orientation of the rigid body are

$$\begin{bmatrix} \dot{\varphi} \\ \dot{\theta} \\ \dot{\psi} \end{bmatrix} = \frac{1}{\cos \theta} \begin{bmatrix} \cos \theta & \sin \theta \sin \varphi & \sin \theta \cos \varphi \\ 0 & \cos \theta \cos \varphi & -\cos \theta \sin \varphi \\ 0 & \sin \varphi & \cos \varphi \end{bmatrix} \begin{bmatrix} p \\ q \\ r \end{bmatrix}$$

$$\mathbf{R}(\varphi, \theta, \psi) = \begin{bmatrix} c_{\theta} c_{\psi} & c_{\theta} s_{\psi} & -s_{\theta} \\ s_{\varphi} s_{\theta} c_{\psi} - c_{\varphi} s_{\psi} & s_{\varphi} s_{\theta} s_{\psi} + c_{\varphi} c_{\psi} & s_{\varphi} c_{\theta} \\ c_{\varphi} s_{\theta} c_{\psi} + s_{\varphi} s_{\psi} & c_{\varphi} s_{\theta} s_{\psi} - s_{\varphi} c_{\psi} & c_{\varphi} c_{\theta} \end{bmatrix}$$

## The phenomenon of gimbal lock

A singularity in the system of differential equations occurs when the pitch angle  $\theta = \pm 90^{\circ}$  (nose up/down)

$$\mathbf{R}(\varphi, \theta, \psi) = \begin{bmatrix} 0 & 0 & -1 \\ -\sin(\psi - \varphi) & \cos(\psi - \varphi) & 0 \\ \cos(\psi - \varphi) & \sin(\psi - \varphi) & 0 \end{bmatrix}$$

$$\mathbf{R}(\varphi, \theta, \psi) = \begin{bmatrix} 0 & 0 & 1 \\ -\sin(\psi + \varphi) & \cos(\psi + \varphi) & 0 \\ -\cos(\psi + \varphi) & -\sin(\psi + \varphi) & 0 \end{bmatrix}$$

## Kinematic differential equations

### ➤ Formulation of the differential equations system

It depends on the parameterization used to describe the attitude

$$\begin{bmatrix} \dot{\phi} \\ \dot{\theta} \\ \dot{\psi} \end{bmatrix} = \frac{1}{\cos\theta} \begin{bmatrix} \cos\theta & \sin\theta \sin\varphi & \sin\theta \cos\varphi \\ 0 & \cos\theta \cos\varphi & -\cos\theta \sin\varphi \\ 0 & \sin\varphi & \cos\varphi \end{bmatrix} \begin{bmatrix} p \\ q \\ r \end{bmatrix}$$

$$\begin{bmatrix} \dot{C}_{11} & \dot{C}_{12} & \dot{C}_{13} \\ \dot{C}_{21} & \dot{C}_{22} & \dot{C}_{23} \\ \dot{C}_{31} & \dot{C}_{32} & \dot{C}_{33} \end{bmatrix} = \begin{bmatrix} C_{11} & C_{12} & C_{13} \\ C_{21} & C_{22} & C_{23} \\ C_{31} & C_{32} & C_{33} \end{bmatrix} \begin{bmatrix} 0 & -r & q \\ r & 0 & -p \\ -q & p & 0 \end{bmatrix}$$

## A mention to quaternions – 1

- Euler's theorem states that the most general motion of a rigid body with one point fixed is a rotation by angle  $\phi$  about some axis, i.e., the unit vector  $\mathbf{e}$ .
- A unit quaternion has a three-vector part and a scalar part, which are related to the axis and angle of rotation by

$$\mathbf{q} = \begin{bmatrix} q_0 \\ \mathbf{q} \end{bmatrix} = \begin{bmatrix} \cos(\phi/2) \\ \mathbf{e} \sin(\phi/2) \end{bmatrix} \leftarrow \begin{array}{l} \text{Unit-norm constraint} \\ \sqrt{\|\mathbf{q}\|^2 + q_0^2} = 1 \end{array}$$

## A mention to quaternions – 2

➤ The quaternion representation is 2:1, since  $\mathbf{q}$  and  $-\mathbf{q}$  represents the same DCM (redundancy).

➤ **Kinematic formulation**

$$\begin{bmatrix} \dot{q}_0 \\ \dot{q}_1 \\ \dot{q}_2 \\ \dot{q}_3 \end{bmatrix} = \frac{1}{2} \begin{bmatrix} 0 & -p & -q & -r \\ p & 0 & r & -q \\ q & -r & 0 & p \\ r & q & -p & 0 \end{bmatrix} \begin{bmatrix} q_0 \\ q_1 \\ q_2 \\ q_3 \end{bmatrix}$$

## A mention to quaternions – 3

➤ The DCM is a homogeneous quadratic function of the components of a unit quaternion:

$$\mathbf{A}(\mathbf{q}) = (q_0^2 - \|\mathbf{q}\|^2) \mathbf{I}_{3 \times 3} - 2q_4 \begin{bmatrix} 0 & -q_3 & q_2 \\ q_3 & 0 & -q_1 \\ -q_2 & q_1 & 0 \end{bmatrix} + 2\mathbf{q}\mathbf{q}^T$$

➤ Most quaternion estimation methods are based on (Extended) Kalman filtering.

## The acceleration vector – 1

### Theoretical development

The acceleration of a point  $P$  on a rigid body is

$$\mathbf{a}_P = \ddot{\mathbf{R}} + \mathbf{g} + \boldsymbol{\omega} \times (\boldsymbol{\omega} \times \mathbf{p}) + \dot{\boldsymbol{\omega}} \times \mathbf{p}$$

$\ddot{\mathbf{R}}$ : acceleration of the body-fixed frame w.r.t the inertial frame

$\mathbf{a}$ : acceleration of the point  $P$  relative to the body-fixed frame

$\boldsymbol{\omega}$ : angular velocity of the body

$\dot{\boldsymbol{\omega}}$ : angular acceleration of the body

$\mathbf{v}$ : velocity of the point  $P$  relative to the body-fixed frame

$\mathbf{P}$ : position vector of the point  $P$  from the origin of the body fixed frame

$\mathbf{g}$ : gravitational field

## The acceleration vector – 2

### Theoretical development

The acceleration of a point  $P$  on a body is

$$\mathbf{a}_P = \ddot{\mathbf{R}} + \mathbf{g} + \mathbf{a} + 2 \boldsymbol{\omega} \times \mathbf{v} + \boldsymbol{\omega} \times (\boldsymbol{\omega} \times \mathbf{p}) + \dot{\boldsymbol{\omega}} \times \mathbf{p}$$

Assumptions:

1. Rigid body
2. The point  $P$  is the origin of the body frame

$$\mathbf{a}_P = \ddot{\mathbf{R}} + \mathbf{g}$$

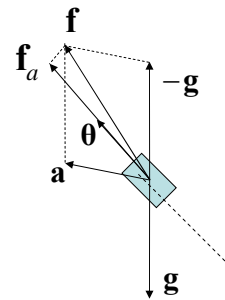
## Accelerometer output equation – 1

A single-axis accelerometer mounted on a rigid body is a device with one input and one output that measures the force, *per unit mass*, acting on the body

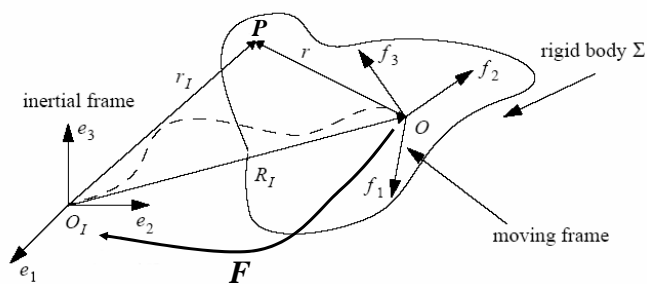
$$\mathbf{f} = \mathbf{a} - \mathbf{g}$$

along a specific sensing direction  $\theta$ :

$$f_a = (\mathbf{a} - \mathbf{g}) \cdot \theta$$



## Accelerometer output equation – 2



$$r_I = R_I + r = R_I + F u$$

$$\ddot{r}_I = \ddot{R}_I + \ddot{F} u = \ddot{R}_I + F(\dot{\Omega} + \Omega^2)u$$

$$\Omega = \begin{bmatrix} 0 & -\omega_z & \omega_y \\ \omega_z & 0 & -\omega_x \\ -\omega_y & \omega_x & 0 \end{bmatrix}$$

$$f_a = (\ddot{R}_I - g + F(\dot{\Omega} + \Omega^2)u) \cdot (F\theta) = \\ = (F^T(\ddot{R}_I - g)) \cdot \theta$$

# Strap-down inertial navigation in human movement analysis

## Strap-down INS

The accelerometers and gyros are mounted in body coordinates and are not mechanically moved.

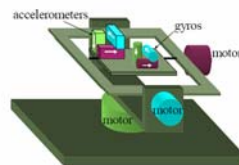


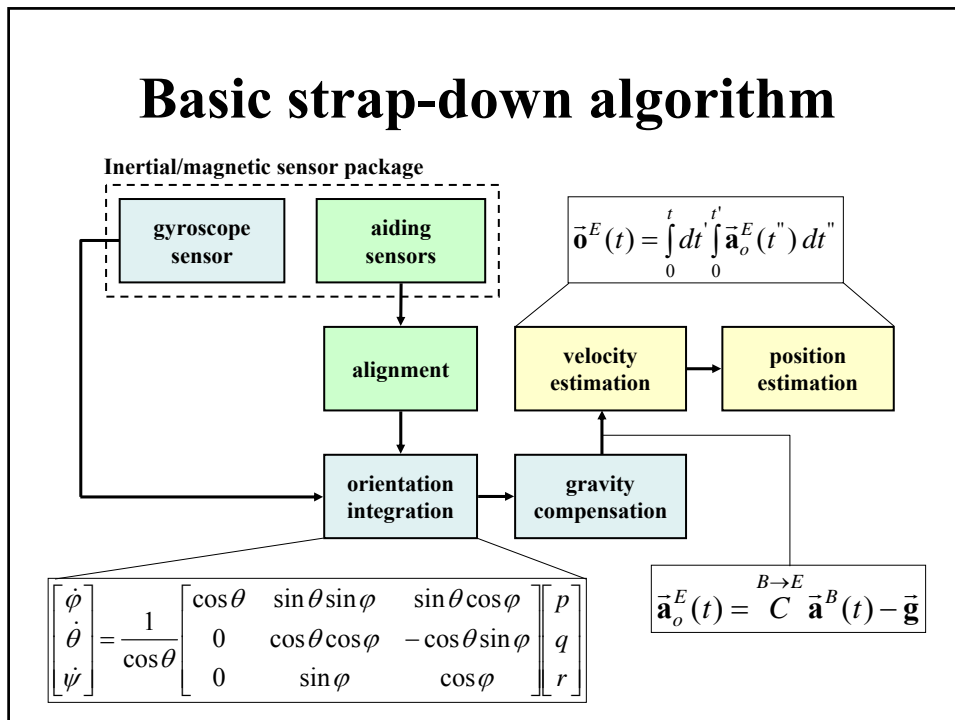
Figure 2a : Stable platform INS



Figure 2b: Strapdown INS

A computer solution is used to keep track of the IMU orientation and to rotate the measurements from the body frame to the navigational frame.

# Basic strap-down algorithm



## Comments – 1

### ➤ Orientation estimation

The problem with tracking orientation using only gyros is drift. Main factors involved:

- ✓ gyro bias and gyro bias instability
- ✓ gyro white noise
- ✓ gyro calibration errors

will be discussed later on.

## Comments – 2

### ➤ **How to solve the problem of gyro drift**

- ✓ Use higher accuracy sensors and algorithms to keep the drift rate low
- ✓ Require the user to return to a known position/orientation and restart after a certain period of time.

## Comments – 3

### ➤ **Principles of complementary filtering**

Use additional sensors:

- ✓ Gravimetric tilt sensing (pitch and roll drift stabilization)
- ✓ Earth's magnetic sensing (yaw drift stabilization)

### ➤ **Open problems**

- ✓ How to prevent slosh in gravimetric tilt sensing
- ✓ How to prevent effects of magnetic disturbances

## Comments – 4

### ➤ **Position estimation**

Drift in the linear position determined by an INS arises from several sources:

- ✓ accelerometer bias and bias instability
- ✓ accelerometer white noise
- ✓ accelerometer calibration errors
- ✓ orientation error in gravity compensation

### ➤ **Open problems**

- ✓ Nightmare of the double-integration

## Gyro-free IMUs

Availability of inexpensive solid state sensors, e.g., accelerometers and magnetic sensors.

Their main limitations are:

- ✓ They are generally not capable of providing high-bandwidth orientation information.
- ✓ They cannot generate a valid orientation solution during certain rigid body movements.

## **All-accelerometer IMUs**

It is possible to determine the angular velocity and acceleration of a rigid-body by measuring the acceleration of different points of the body.

Their main limitations are:

- ✓ The body angular velocity is (generally) computed by integrating the angular acceleration.
- ✓ It is critical the problem of sensor placement (position and orientation of the sensitive axes).

## **Sensor modeling and calibration: gyro and accelerometers**

## Uni-axis gyro model

Equation that gives the rate gyro output  $u_g$  as a function of the angular velocity component  $\omega_s$  directed along the sensor sensitivity axis:

$$u_g = k_g \omega_s + d_{g,a} + b_g$$

Rate gyro scale factor, mV/°/s      Rate gyro bias, mV

Effect of the linear acceleration on the rate gyro, mV/m/s<sup>2</sup>

## Tri-axis gyro model

Equation that gives the rate gyro output  $\mathbf{u}_g$  as a function of the angular velocity  $\boldsymbol{\omega}_s$ :

$$\mathbf{u}_g = \mathbf{K}_g \mathbf{R}_g \boldsymbol{\omega}_s + \mathbf{d}_{g,a} + \mathbf{b}_g$$

Scale factor matrix

$$\mathbf{K}_g = \begin{bmatrix} k_{gx} & 0 & 0 \\ 0 & k_{gy} & 0 \\ 0 & 0 & k_{gz} \end{bmatrix}$$

Misalignment error

$$\mathbf{R}_g = \begin{bmatrix} r_{11} & r_{12} & r_{13} \\ r_{21} & r_{22} & r_{23} \\ r_{31} & r_{32} & r_{33} \end{bmatrix}$$

## Acceleration sensitivity

➤ **Definition**

The inner product between the vector  $\mathbf{k}_{g,a}$ , which expresses the sensitivity components along three Cartesian axes, and the vector  $\mathbf{a}$ , which expresses the acceleration components along the same axes

$$d_{g,a} = \mathbf{k}_{g,a} \cdot \mathbf{a}$$

## Bias

➤ **Definition**

The output component from a rate gyro measured at specified operating conditions, i.e., temperature, that does not have correlation with angular velocity or linear acceleration

$$b_g(t) = b_{g0} + b_{g1}t$$

It consists of components that are systematic (bias offset) and random (bias drift)

## Bias offset and drift

- The output errors tend to be stochastic in nature

$$\begin{bmatrix} \dot{\varphi} \\ \dot{\theta} \\ \dot{\psi} \end{bmatrix} = \frac{1}{\cos \theta} \begin{bmatrix} \cos \theta & \sin \theta \sin \varphi & \sin \theta \cos \varphi \\ 0 & \cos \theta \cos \varphi & -\cos \theta \sin \varphi \\ 0 & \sin \varphi & \cos \varphi \end{bmatrix} \begin{bmatrix} p + b_p \\ q + b_q \\ r + b_r \end{bmatrix}$$

- **Error model**

Constant null-shift  $\rightarrow$   $b_0$  Band-limited white noise, with variance  $\sigma_{w1}^2$   $\rightarrow$   $b_w(t)$

$$b(t) = b_0 + b_1(t) + b_w(t)$$

$\uparrow$   
Time-varying component (exponentially correlated Gaussian random process with variance  $\sigma_{b1}^2$  and correlation time  $\tau$ ).

$$\dot{b}_1(t) = -\frac{1}{\tau} b_1(t) + w_{b1}$$

## Uni-axis accelerometer model

Equation that gives the accelerometer output  $u_a$  as a function of the acceleration component  $a_s$  directed along the sensor sensitivity axis:

Accelerometer scale factor, mV/m/s<sup>2</sup>

$$u_a = k_a a_s + b_a$$

Accelerometer bias, mV

## Tri-axis accelerometer model

Equation that gives the accelerometer output  $\mathbf{u}_a$  as a function of the acceleration  $\mathbf{a}_s$ :

$$\mathbf{u}_a = \mathbf{K}_a \mathbf{R}_a \mathbf{a}_s + \mathbf{b}_a$$

Scale factor matrix

$$\mathbf{K}_a = \begin{bmatrix} k_{ax} & 0 & 0 \\ 0 & k_{ay} & 0 \\ 0 & 0 & k_{az} \end{bmatrix}$$

Misalignment error

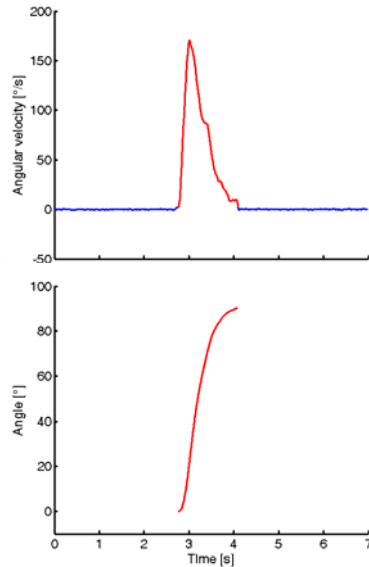
$$\mathbf{R}_a = \begin{bmatrix} r_{11} & r_{12} & r_{13} \\ r_{21} & r_{22} & r_{23} \\ r_{31} & r_{32} & r_{33} \end{bmatrix}$$

## Gyro calibration – 1

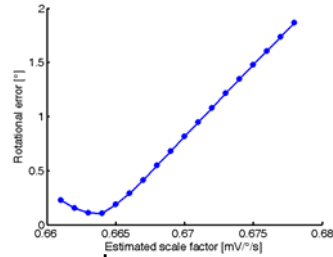
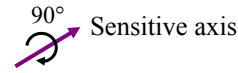
- The bias offset determination is greatly simplified, especially in the case that low-cost, low-resolution sensors are considered
- Example
  - ✓ Earth's rotation:  $15^\circ/\text{h} - 0.0042^\circ/\text{s}$
  - ✓ Scale factor:  $2\text{mV}/^\circ/\text{s}$  (typical value)
  - ✓ Resolution required:  $8.5\ \mu\text{V}$
  - ✓ A/D resolution:  $80\ \mu\text{V}$  (range:  $2.5\text{V} - 16\ \text{bit}$ )
  - ✓ Standard deviation MEMS gyro:  $0.5^\circ/\text{s}$  (typical value)
- Comment

The bias offset is determined when the gyro is steady, irrespective of the orientation of its sensitive axes

## Gyro calibration – 2



Method of controlled rotations

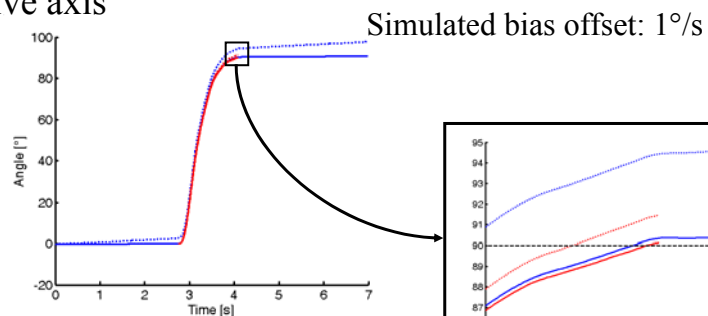


$$S_v = 0.664 \text{ mV}/^\circ/\text{s}$$

$$\hat{\theta} = 89.89^\circ \pm 0.29^\circ$$

## Gyro calibration – 3

Behavior in a controlled rotation of 90° around the sensitive axis



The bias offset is time-integrated and therefore it must be compensated for high accuracy.

## Accelerometer calibration – 1

### ➤ Approach

Two acceleration measurements are performed, before and after a rotation of  $180^\circ$  around a horizontal axis (reverse the gravity effect in the two measurements)

$$\begin{aligned} \mathbf{u}_{a1} &= \mathbf{K}_a \mathbf{R}_a \mathbf{g} + \mathbf{b}_a \\ \mathbf{u}_{a2} &= \mathbf{K}_a \mathbf{R}_a (-\mathbf{g}) + \mathbf{b}_a \end{aligned} \quad \rightarrow \quad \mathbf{b}_a = \frac{\mathbf{u}_{a1} + \mathbf{u}_{a2}}{2}$$

## Accelerometer calibration – 2

### ➤ Perform the measurements with each sensitive axis placed parallel and anti-parallel to gravity

$$\mathbf{U}_{a1} = g \mathbf{K}_a \mathbf{R}_a + \mathbf{B}_a$$

$$\mathbf{U}_{a2} = -g \mathbf{K}_a \mathbf{R}_a + \mathbf{B}_a$$

$$\mathbf{U}_{aS} = \mathbf{U}_{a1} + \mathbf{U}_{a2}$$

$$\mathbf{U}_{aD} = \mathbf{U}_{a1} - \mathbf{U}_{a2}$$

$$\mathbf{B}_a = \frac{1}{2} \mathbf{U}_{aS}$$

$$\mathbf{K}_a \mathbf{R}_a = \frac{1}{2g} \mathbf{U}_{aD}$$

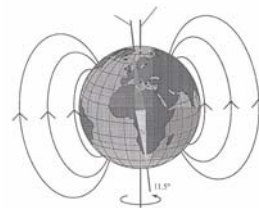
$$\begin{bmatrix} k_{ax} \\ k_{ay} \\ k_{az} \end{bmatrix} = \text{diag}[(\mathbf{K}_a \mathbf{R}_a)(\mathbf{K}_a \mathbf{R}_a)^T] = \frac{1}{4g^2} \text{diag}[\mathbf{U}_{aD} \mathbf{U}_{aD}^T]$$

$$\mathbf{R}_a = \frac{1}{2g} \mathbf{K}_a \mathbf{U}_{aD}$$

## **Sensor modeling and calibration: magnetic sensors**

### **The earth's magnetic field**

➤ Determining direction by measuring geomagnetism using a compass

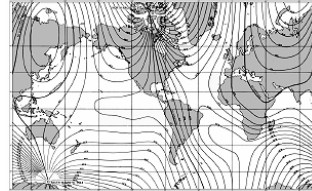


➤ Limitations

- ✓ host platform magnetic field
- ✓ natural or manmade magnetic anomalies
- ✓ variation/inclination of the earth's magnetic field
- ✓ dynamic conditions (accelerations) of the platform

## Using the earth's magnetic field to determine direction – 1

- The local magnetic field varies greatly in intensity and direction over the surface of the earth.

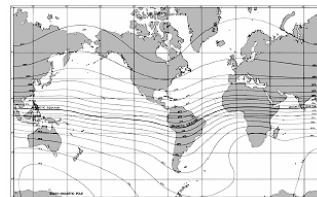


- **Variation**

Difference between the local magnetic meridian and the local geographic meridian at any particular point on the earth.

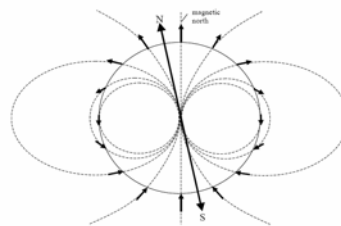
## Using the earth's magnetic field to determine direction – 2

- The local magnetic field varies greatly in intensity and direction over the surface of the earth.



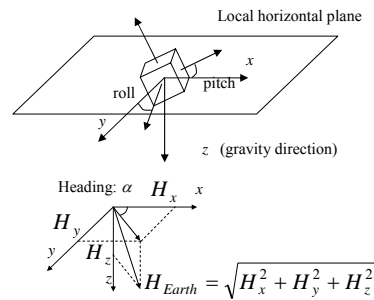
- **Inclination or dip angle**

Angle between the magnetic field and the horizontal component.



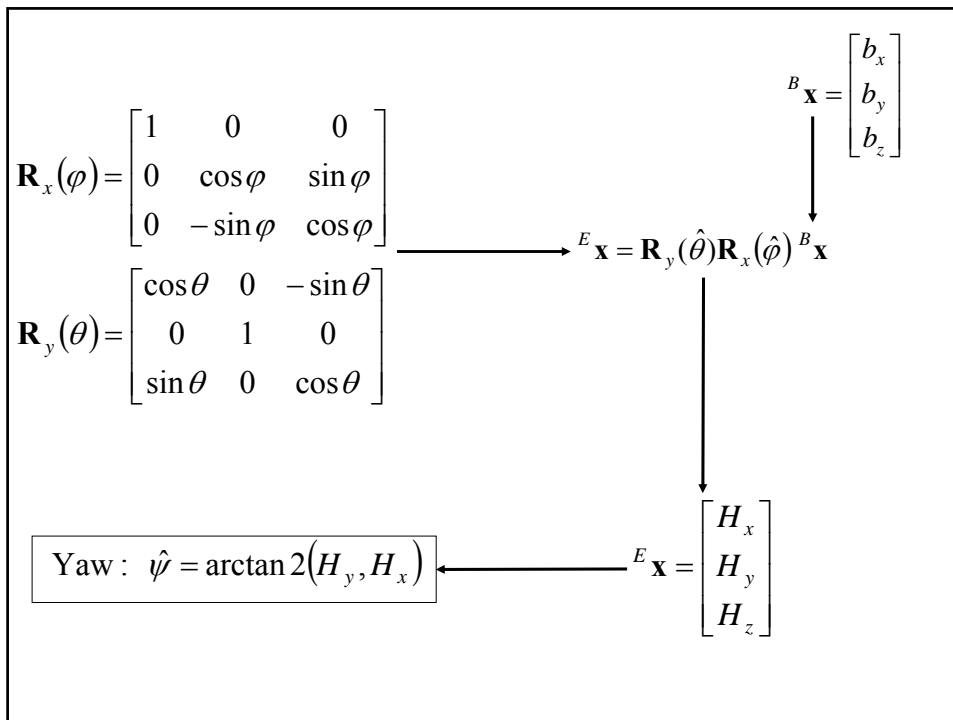
## Tilt determination

- The approach is to rotate the compass orientation to the horizontal plane



- One method to determine the inclination, i.e., the roll and pitch angles, of the sensor case is to use a tilt sensor that senses the direction of gravity.

$$\begin{aligned}
 \mathbf{R}_x(\varphi) &= \begin{bmatrix} 1 & 0 & 0 \\ 0 & \cos \varphi & \sin \varphi \\ 0 & -\sin \varphi & \cos \varphi \end{bmatrix} \\
 \mathbf{R}_y(\theta) &= \begin{bmatrix} \cos \theta & 0 & -\sin \theta \\ 0 & 1 & 0 \\ \sin \theta & 0 & \cos \theta \end{bmatrix} \\
 \mathbf{E}_x &= \begin{bmatrix} 0 \\ 0 \\ g \end{bmatrix} \\
 \mathbf{B}_x &= \mathbf{R}_x(\varphi) \mathbf{R}_y(\theta) \mathbf{E}_x \\
 \begin{bmatrix} a_x \\ a_y \\ a_z \end{bmatrix} &= \begin{bmatrix} -\sin \theta \\ \sin \varphi \cos \theta \\ \cos \varphi \cos \theta \end{bmatrix} g \\
 \text{Pitch: } \hat{\theta} &= -\arcsin\left(\frac{a_x}{g}\right) \\
 \text{Roll: } \hat{\varphi} &= \arctan\left(\frac{a_y}{a_z}\right)
 \end{aligned}$$



## On heading accuracy

$$\Delta \psi = -\Delta \varphi \cdot \tan \delta \cdot \cos \psi - \Delta \theta \cdot \tan \delta \cdot \sin \psi$$

↑  
Dip angle

Caveat:  
Slosh effect on tilt sensing

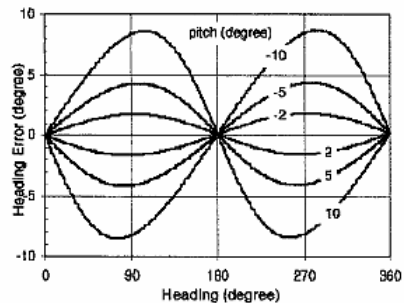


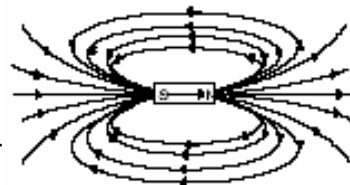
Figure 4—Heading errors due to pitch without tilt compensation (Dip Angle = 40°).

## Effects of magnetic disturbances

- Another consideration for heading accuracy is:
  - ✓ The presence of nearby ferrous materials on the earth's magnetic field
  - ✓ Man-made disturbances (vehicles, buildings, phones)
  - ✓ Natural disturbances (sunspots, solar magnetic storms)
- Magnetic distortions can be categorized as two types – hard iron and soft iron effects.

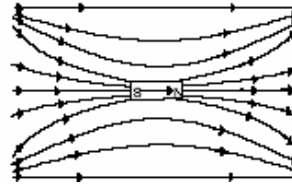
## Hard iron effects

- They arise from permanent magnets and magnetized iron or steel on the compass platform.
- These distortions will remain constant and in a fixed location relative to the compass for all heading orientations.
- Hard iron effects add a constant magnitude field component along each axes of the sensor output.



## Soft iron effects

- They arise from the interaction of the earth's magnetic field and any magnetically soft material surrounding the compass.



- These distortions do not remain constant, they vary with the orientation of the platform relative to the direction of the earth's magnetic field.
- Soft irons change the shape of the measurement locus.

## Measurement 2D-locus

The host platform where a level compass (null inclination) is installed performs a full turn of 360°.

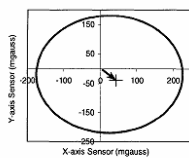


Figure 10—Hard iron offsets when rotated horizontally in the earth's field.

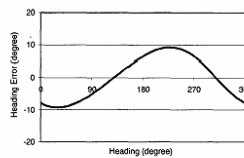


Figure 11—Heading error due to hard iron effects known as single-cycle errors.

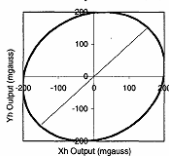


Figure 12—Soft iron distortion when rotated horizontally in the earth's field.

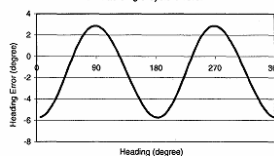


Figure 13—Heading error due to soft iron effects known as two-cycle errors.

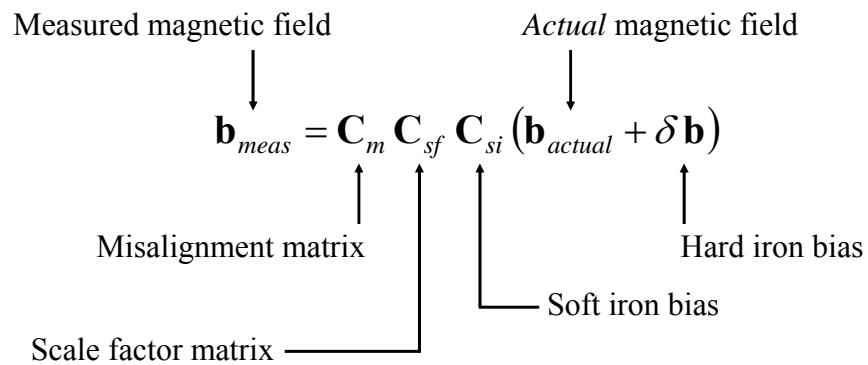
$$\bar{H}_x = (1 + sf_x)H_x + H_{off_x}$$

$$\bar{H}_y = (1 + sf_y)H_y + H_{off_y}$$

$$\text{Yaw} : \hat{\psi} = \arctan 2(\bar{H}_y, \bar{H}_x)$$

## Measurement 3D-locus

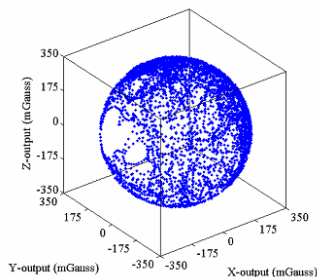
Mathematical model for the output error of a strapdown tri-axis magnetometer



## Method

Non-linear two-step estimation algorithm

$$\sqrt{\left(\frac{b_{meas\ x} - \delta b_x}{1 + sf_x}\right)^2 + \left(\frac{b_{meas\ y} - \delta b_y}{1 + sf_y}\right)^2 + \left(\frac{b_{meas\ z} - \delta b_z}{1 + sf_z}\right)^2} = b_{earth}$$



Possible problems:

Sensitivity to initial guess (scale factors and hard iron biases)

Portion of the complete ellipsoid available for carrying the estimation process, as a function of the measurement noisiness

## **Sensor calibration in HMA – 1**

- Need for sensor calibration *immediately* before use
- Low-cost devices used in *uncontrolled* environments
- Effects of time drifts and sensitivity to environmental parameters, e.g., temperature
- Frequent calibrations needed for body-fixed sensors
- Availability of in-field calibration procedures

## **Sensor calibration in HMA – 2**

- Scale factor drifts are often negligible
- Misalignment is well controlled and compensated for in integrated MEMS IMU
- Effectiveness of thermal compensation
- Importance of the warm-up for thermal stabilization

## **Dead-reckoning approaches for pedestrian navigation systems**

### **Pedestrian navigation systems**

➤ **Definition**

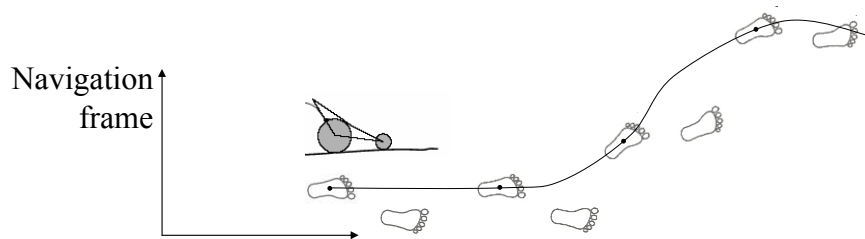
Systems which provide velocity and position of a person wearing the system (any time – any environment)

➤ **Applications**

- ✓ Location-based services (E-911 service)
- ✓ Navigation for the blind
- ✓ Ambulatory monitoring systems

## Dead-reckoning principle

Dead-reckoning relying on wheel-encoders (mobile robotics) and inertial sensing (pedestrian navigation systems, PNS) is widely used to generate position



## Dead-reckoning implementation

- Positioning in indoor/outdoor environments
- GPS technology shortcomings:
  - ✓ no static heading;
  - ✓ lack of availability of satellite signals;
  - ✓ power consumption
- Interest for technologies which do not require environment structuring (indoor applications)
- Interest for technologies which help overcome GPS limitations (outdoor applications)

## **Pedestrian mechanization**

- **Approach: ad-hoc strap-down INS**  
Restrict error growth by propagating position estimates in a stride-wise fashion.
- **What to be detected/estimated?**
  - ✓ Step detection
  - ✓ Stride length estimation
  - ✓ Heading determination

## **Stride and heading determination**

- **Zero velocity update**  
The integration of acceleration measurements is only performed during the swing of legs and the velocity errors are reset with each step.
- **Stride-by-stride alignment**
  - ✓ Gravimetric tilt sensing / geomagnetic compassing is safely used when the IMU is known to be steady
  - ✓ Gyro bias capture occasionally performed to compensate for the gyro bias offset.

## Stride and heading determination

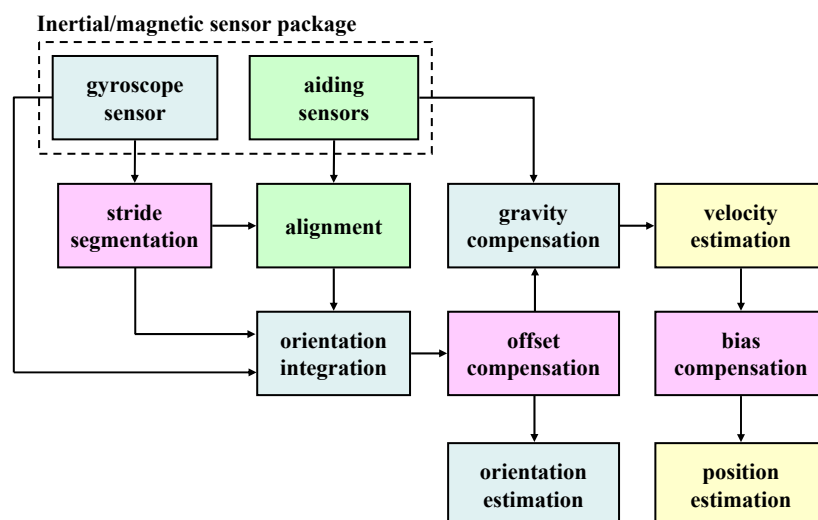
### ➤ Strap-down integral reset

The integration of gyroscopic measurements is performed on a stride-by-stride mode.

### ➤ In-line compensation of sensor errors

- ✓ Maintaining heading is critical.
- ✓ Role of (Extended) Kalman filters.

## Basic strap-down algorithm

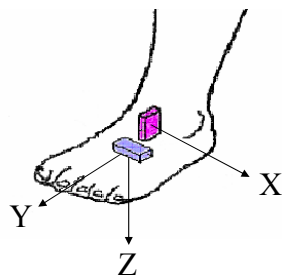


## Shoe- or waist-mounted PNS ?

### ➤ Optimal sensor placement

- ✓ Where the dynamics of human movement is less challenging
- ✓ Where the velocity of body part is less influenced by body sway (zero-velocity update)
- ✓ Where the stride length can be measured
- ✓ Where the heading can be estimated

## Shoe-mounted PNS



The IMU is composed of two bi-axis accelerometer and one uni-axis gyro

a) Accelerometers (Analog Devices ADXL210E)

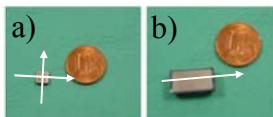
Sensitivity: 100 mV/g ( $g = 9.81 \text{ m/s}^2$ )

Sensing range:  $\pm 10 \text{ g}$

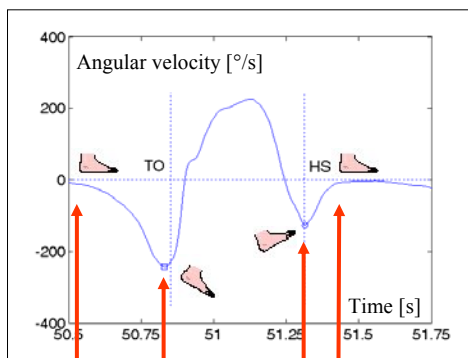
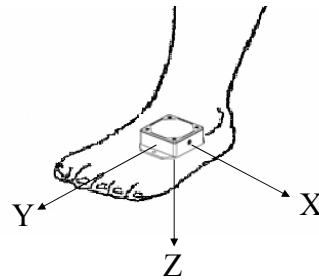
b) Gyro (Murata ENC-03J)

Sensitivity: 2.5 mV/°/s

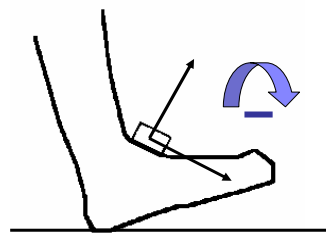
Sensing range:  $\geq 400 \text{ }^\circ/\text{s}$



Orientation Range	360 degrees full scale (FS), all axes (Matrix, Quaternion modes)
Sensor Range	Gyros: +/-300 degrees/sec FS; accelerometers: +/- 5 G's FS; magnetometers: +/-1.2 Gauss FS
A/D Resolution	16 bits
Accelerometer Nonlinearity	0.2%
Accelerometer Bias Stability*	0.010 G's
Gyro Nonlinearity	0.2%
Gyro Bias Stability*	0.7 degrees/sec
Magnetometer Nonlinearity	0.4%
Magnetometer Bias Stability*	.010 Gauss
Orientation Resolution	< 0.1 degrees minimum
Repeatability	0.20 degrees
Accuracy	+/-0.5 degrees typical for static test conditions, +/-2 degrees typical for dynamic (cyclic) test conditions and for arbitrary orientation angles
Output Modes	Matrix, Quaternion, Euler angles and 9 scaled sensors with temperature
Digital Outputs	Serial RS-232 and RS-485 optional with software programming
Analog Output Option	0-5 volts FS for Euler angles (pitch +/-90, roll +/-180, yaw 360 dep.)
Digital Output Rates	100 Hz for Euler, Matrix, Quaternion; 350 Hz for 9 orthogonal sensors only
Serial Data Rate	19.2/38.4/115.2 Kbaud, software programmable
Supply Voltage	5.2 VDC min., 12 VDC max.
Supply Current	65 milliamps
Connectors	One keyed LEMO, two for RS-485 option
Operating Temperature	-40 to +70 degrees Celsius with enclosure; -40 to +85 degrees Celsius without enclosure
Size with Enclosure	65 x 90 x 25 mm; 2.5 x 3.5 x 1.0"
Size without Encl.	42 x 40 x 15 mm; 1.65 x 1.6 x 0.6"
Weight	74.6 gr. with enclosure, 25.8 gr. without enclosure
Shock Limit	1000 G's (unpowered); 500 G's (powered)



## Step detection



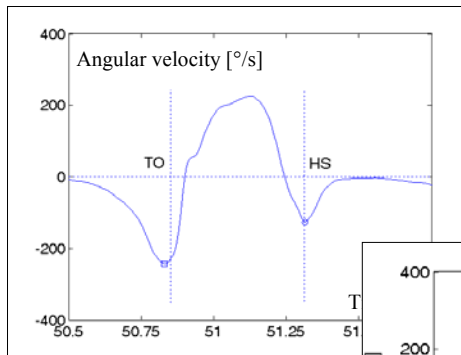
Transition: *heel-strike* → *stance*  $|\dot{\theta}| \leq TH_{FS}$

Transition: *swing* → *heel strike (HS)*

Transition: *heel-off* → *swing*, event detected: *toe-off (TO)*

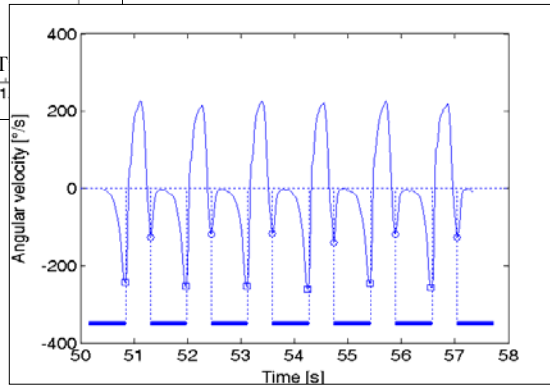
Transition: *stance* → *heel-off*  $|\dot{\theta}| \geq TH_{HO}$

Sabatini, A.M., Martelloni, C., Scapellato, S., Cavallo, F. (2005). Assessment of walking features from foot inertial sensing. *IEEE Trans. Biomed. Eng.*, 52, pp.486-494.



FSR footswitches, placed underneath the heel and the big toe, can be used as reference standard to confirm the validity of the gait phase detection.

The toe-off event is estimated by the foot gyroscope with a small bias as compared with the FSR indication (about 35 ms); the heel strike detection is unbiased

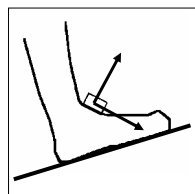
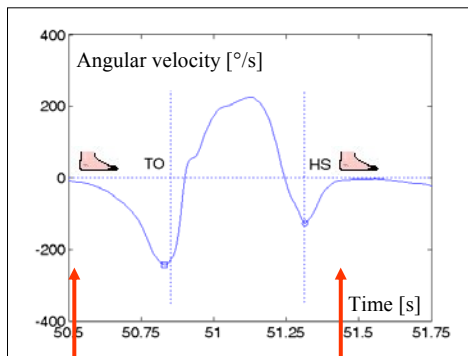


## Alignment

### Zero velocity update technique

Aim: to correct the gyroscope-induced orientation error

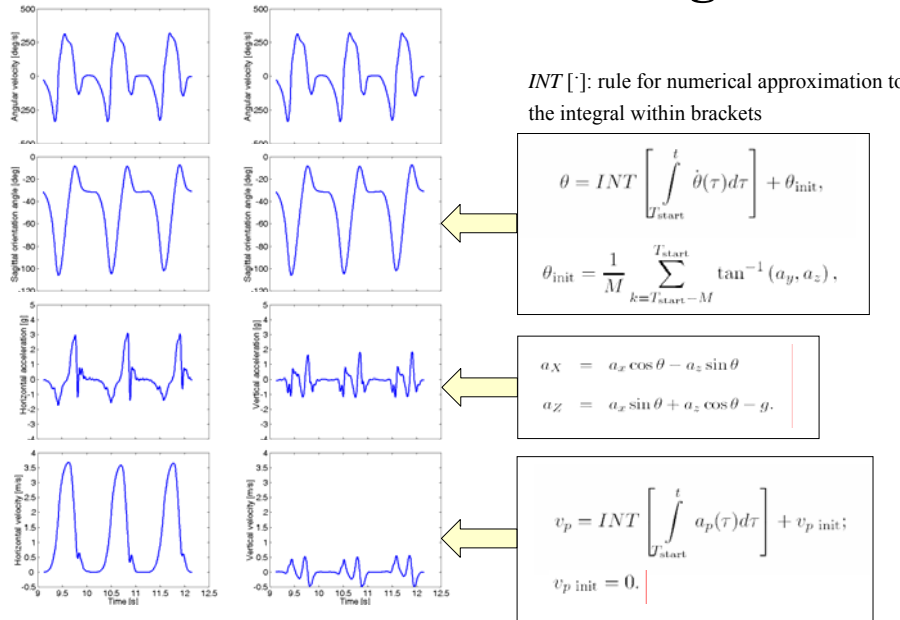
Provided that the foot is at rest during stance, the accelerometers can sense the orientation of the gravity acceleration vector



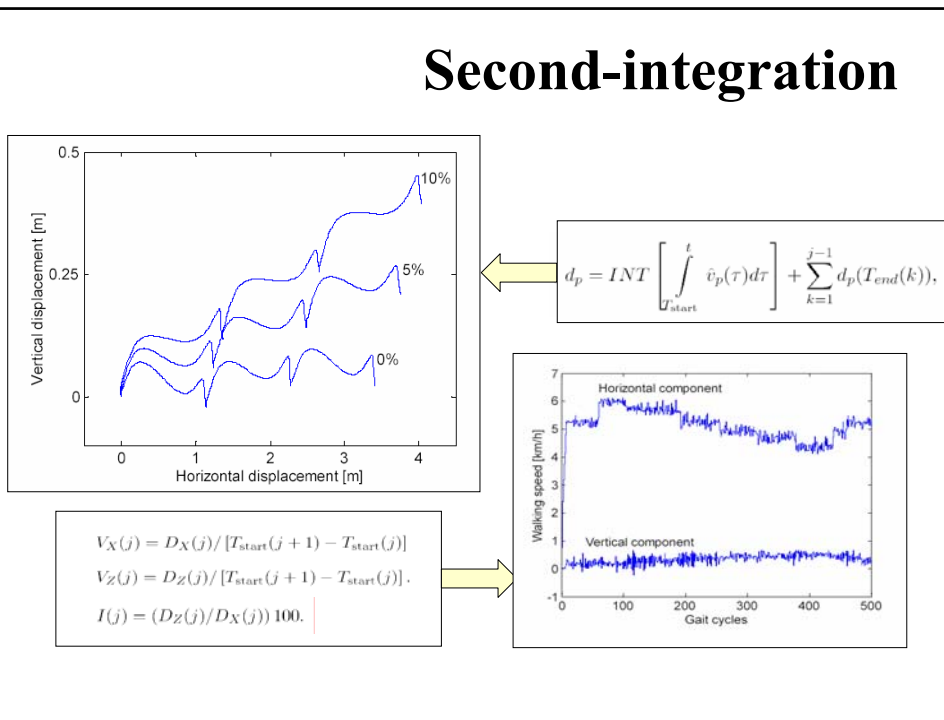
Transition: *heel-strike* → *stance*

Transition: *stance* → *heel off*

# First-integration



# Second-integration



## Indirect estimation of stride length

### ➤ Adoption of pendular models of walking

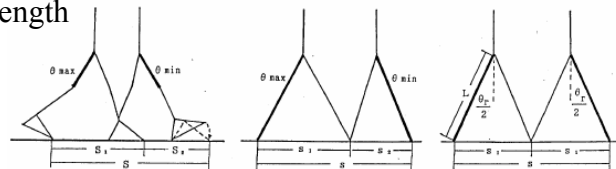
- ✓ Use sensor signals to determine how many steps are taken and then multiply the number of step by the average step length
- ✓ Exploitation of the knowledge that a good correlation exists between the step length and the step frequency
- ✓ How to detect changes in walking conditions that would invalidate the model



## Some examples – 1

### Thigh gyro (Miyazaki, 1997)

1. Assume a symmetric single-segment gait model
2. Measure the extended leg length
3. Compute the peak-to-peak value of the integrated gyro output signal
4. Estimate the stride length

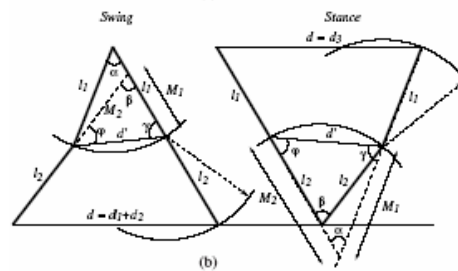
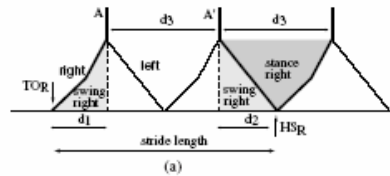


$$s = s_1 + s_2 = 2 \cdot 2L \sin\left(\frac{\theta_{\max} - \theta_{\min}}{2}\right)$$

## Some examples – 2

**Thigh and shank gyros** (Aminian et al., 2002)

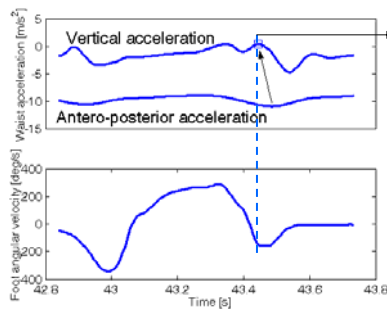
1. Assume a symmetric double-segment gait model
2. Measure the thigh and shank leg lengths
3. Estimate the distance during stance and swing phases



## Some examples – 3

**Waist accelerometers** (Fang et al., 2005)

1. Assume a symmetric single-segment gait model
2. Perform user-specific calibration (determine the constant  $K$ )
3. Compute the peak-to-peak value of the vertical acceleration signal



$$s = s_1 + s_2 = 4\sqrt{A_{\max} - A_{\min}} \cdot K$$

## Performance comparison

➤ **Approach A**  
(foot features)

- ✓ Gyro-based
- ✓ segmentation
- ✓ Strap-down integration

➤ **Approach B and C**  
(waist features)

- ✓ Accelerometer-based segmentation
- ✓ Calibration of models relating walking speed and RMS acceleration norm (approach B) and trunk vertical displacement (approach C)

RMSE of predicted vs. nominal walking speed (treadmill) [m/s]

	$V_H - A$	$V_V - A$	$V_H - B$	$V_H - C$
Subject 1	0.059	0.065	0.082	0.095
Subject 2	0.056	0.031	0.054	0.016
Subject 3	0.045	0.057	0.033	0.038
Subject 4	0.033	0.058	0.091	0.048

## Treadmill walking

➤ **Subject selection**

Five healthy male individuals  
(age:  $30 \pm 7$  ys., height:  $1.80 \pm 0.06$  m, weight:  $79 \pm 7$  kg)

➤ **Walking trials**

On a treadmill (Technogym, Runrace HC1200):

- ✓ Seven speeds  $V_t$ : from 3 km/h to 6 km/h in steps of 0.5 km/h;
- ✓ Five inclines  $I_t$ : -5%, 0%, 5%, 10%, 15%;
- ✓ Trials lasting 2 min at each combination  $V_t$ - $I_t$

➤ **Statistical analysis**

Data from the gait cycles inside the interval [50, 110] s of each trial used to compute  $V_m$  and  $I_m$ .  $V_m$  and  $I_m$  compared with  $V_t$  and  $I_t$  to yield the measurement accuracy in terms of root mean square errors (RMSE).

## RMSE-based performance analysis

	S1	S2	S3	S4	S5
Speed [km/h]	0.16	0.17	0.19	0.09	0.08
Incline [%]	1.27	1.04	1.03	1.23	0.84

## Performance assessment (ground walking)



Experiments performed in different days and conditions.

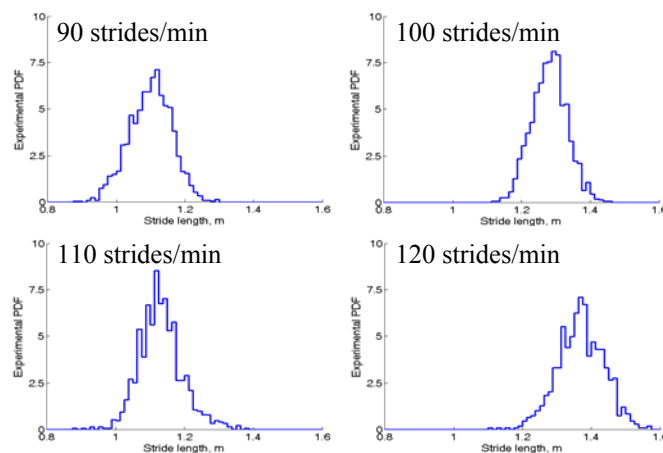
Five 400 m-long trials, at each of four cadence.

Computer-generated beep, used to impose the pace of walking.

Annotation at selected way-points.

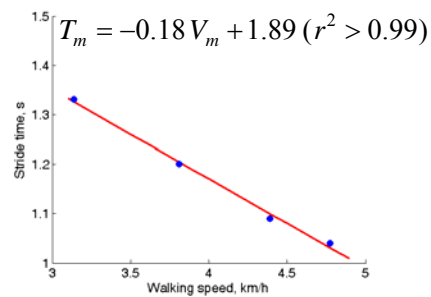
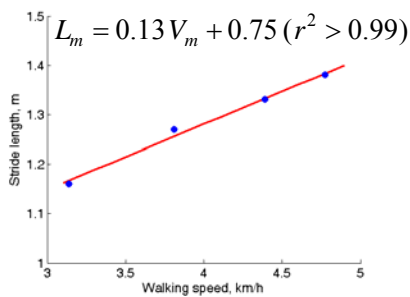
## Experimental results – 1

Statistical analysis of stride variability



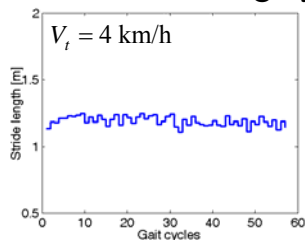
## Experimental results – 2

Cadence, strides/min	90	100	110	120
Stride length, m	$1.16 \pm 0.06$	$1.27 \pm 0.04$	$1.33 \pm 0.05$	$1.38 \pm 0.04$
Stride time, s	$1.33 \pm 0.08$	$1.20 \pm 0.08$	$1.09 \pm 0.08$	$1.04 \pm 0.09$
Walking speed, km/h	$3.17 \pm 0.25$	$3.82 \pm 0.25$	$4.43 \pm 0.40$	$4.82 \pm 0.47$
Distance, m – IMU	$398 \pm 2$	$401 \pm 3$	$403 \pm 6$	$402 \pm 3$
Distance, m – GPS	$407 \pm 4$	$404 \pm 2$	$404 \pm 3$	$397 \pm 3$



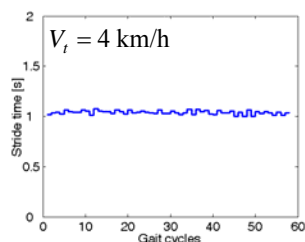
## Experimental results – 3

Treadmill walking by the same subject



Five speeds  $V_t$  tested, from 3 km/h to 5 km/h  
in steps of 0.5 km/h

Results of the regression analysis:



$$L_m = 0.14 V_m + 0.69 (r^2 > 0.99)$$

$$L_m = 0.13 V_t + 0.75 (r^2 > 0.99)$$

$$T_m = -0.17 V_m + 1.83 (r^2 > 0.99)$$

$$T_m = -0.15 V_t + 1.78 (r^2 > 0.99)$$

## Experimental results – 4

### GROUND WALKING

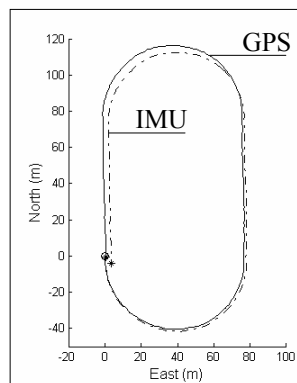
Cadence, strides/min	90	100	110	120
Stride length, m	$1.16 \pm 0.06$	$1.27 \pm 0.04$	$1.33 \pm 0.05$	$1.38 \pm 0.04$
Stride time, s	$1.33 \pm 0.08$	$1.20 \pm 0.08$	$1.09 \pm 0.08$	$1.04 \pm 0.09$
Walking speed, km/h	$3.17 \pm 0.25$	$3.82 \pm 0.25$	$4.43 \pm 0.40$	$4.82 \pm 0.47$

### TREADMILL WALKING

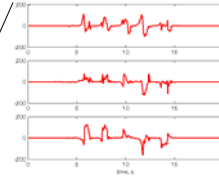
Cadence, strides/min	88	105	111	115
Treadmill speed, km/h	3	3.5	4	4.5
Stride length, m	$1.15 \pm 0.05$	$1.24 \pm 0.02$	$1.30 \pm 0.02$	$1.42 \pm 0.03$
Stride time, s	$1.36 \pm 0.05$	$1.14 \pm 0.03$	$1.08 \pm 0.02$	$1.05 \pm 0.02$
Walking speed, km/h	$3.06 \pm 0.11$	$3.92 \pm 0.08$	$4.35 \pm 0.07$	$4.89 \pm 0.11$

## Experimental results – 5

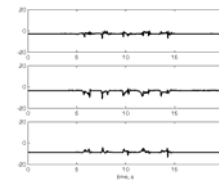
GPS-based heading estimates used to provide IMU-based path reconstruction



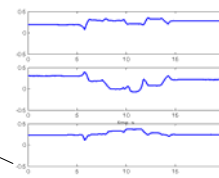
## 3D trajectory reconstruction



Angular rate, °/s

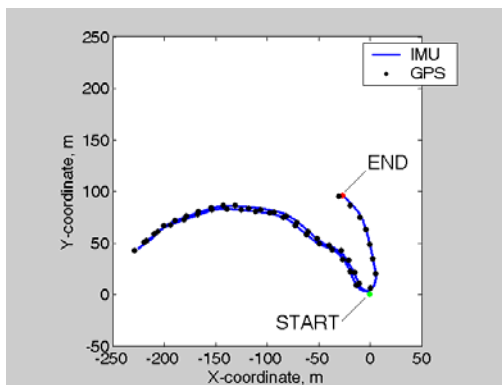


Acceleration, m/s<sup>2</sup>



Magnetic field, Gauss

## Walking in outdoors



### Fourteen-min walk

route length: ~ 680 m

altitude range: ~ 40 m

### Navigation algorithm

Quaternion-based EKF with in-line compensation of magnetic errors

### Calibrated sensors?

	YES	NO
Horizontal displacement error, m:	2.1	12.8
Vertical displacement error, m:	3.4	16.3
Total displacement error, m:	4.0 (< 1%)	20.7 (> 3%)
Error growth rate, mm/s:	6.4	26.2